Available online at www.sciencedirect.com
ScienceDirect
International Journal of Mass Spectrometry 258 (2006) 142–150
International Journal of Mass Spectrometry
www.elsevier.com/locate/ijms

Impact of biomass emissions on particle chemistry during the California Regional Particulate Air Quality Study

Xueying Qin, Kimberly A. Prather *

Department of Chemistry and Biochemistry, University of California, San Diego, 9500 Gilman Drive, La Jolla, CA 92093-0314, United States

Received 1 July 2006; received in revised form 31 August 2006; accepted 1 September 2006

Abstract

This paper describes aerosol time-of-flight mass spectrometry (ATOFMS) measurements of the size and chemical composition of individual particles during the California Regional Particulate Air Quality Study (CRPAQS) (December 2000–February 2001). In Fresno, biomass particles display distinct diurnal variations, peaking at night and reaching a minimum during the day. These biomass particles are small ($D_a \leq 1.0$ μm) and comprise 25% of the total analyzed particles with fractions ranging from 5% during the day to more than 60% at night. In addition, a unique collection of high mass organic carbon (HMOC) particles was identified with similar diurnal variations. The HMOC particles contain characteristic peaks between mass-to-charge (m/z) 100 and 200 in both the positive and negative ion mass spectra. HMOC particles only appear at night and have larger aerodynamic diameters ($D_a \leq 1.0$ μm). Furthermore, the HMOC particles show fragment ions of organic carbon, aromatic compounds, as well as non-mineral potassium, levoglucosan, and marker ions indicative of fog processing. We hypothesize the observed diurnal variations are due to an increase in direct biomass emissions followed by gas/particle partitioning of semivolatile species which undergo aqueous phase processing at night.

Keywords: Organic carbon; Mass spectrometry; Biomass; HULIS; Fog

1. Introduction

The San Joaquin Valley (SJV) is located in central California with mountains on three sides. Pollutants are trapped in the valley due to the secluded geographic features [1], which leads to a deterioration of the air quality. During the winter, $PM_{2.5}$ and PM_{10} concentrations reach their highest in urban areas when multiple sources simultaneously contribute to the aerosol concentrations [2]. Furthermore, secondary ammonium nitrate and carbonaceous species represented the two largest constituents of the PM in the SJV during the winter [2,3]. In atmospheric studies, carbonaceous particulate matter is typically categorized into organic carbon (OC) and elemental carbon (EC). Elemental carbon is the product of incomplete combustion [4], and diesel exhaust is one of the largest EC sources in the SJV [5]. Fine particulate organic carbon concentrations are dominated by biomass burning emissions in winter time in Fresno based on source apportionment using chemical mass balance receptor models [6]. Therefore biomass burning is one of the most important sources of ambient aerosols in the SJV during the winter months.

The wintertime meteorological conditions in SJV are very different from other seasons. Mixing depth and ventilation are low and accompanied by the highest relative humidity (RH) of all seasons [7]. The low mixing depth favors the accumulation of primary emissions. High relative humidities lead to aqueous phase processing of the primary aerosol particles, changing the aerosol composition [8,9]. Therefore, the composition of SJV ambient aerosols is fairly complex during the winter and strongly affected by the liquid water content of the aerosol.

While ammonium nitrate in the SJV has been intensively studied during the last decade [7,10–13], less is known about the components making up the carbonaceous fraction of the aerosols, in particular the semivolatile organic compounds. The formation mechanisms, chemical reactions, and concentrations of organic compounds in the atmosphere are far less understood than other inorganic species, such as sulfate and nitrate [14]; thus, understanding the emission sources, particle transport, and

* Corresponding author. Tel.: +1 858 822 5312; fax: +1 858 534 7042.
E-mail address: kprather@ucsd.edu (K.A. Prather).

1387-3806/$ – see front matter © 2006 Published by Elsevier B.V.
doi:10.1016/j.ijms.2006.09.004

mechanisms of chemical reactions of organics in particulate matter will further our understanding of a variety of atmospheric phenomena [15], which will ideally allow for the development of policies to help alleviate air pollution problems.

Organic compounds are most frequently measured using filter and/or impactor based bulk analysis techniques. While providing valuable information, these techniques require off-line analysis and have several limitations. First, bulk analysis techniques usually require extended collection periods (hours to days) in order to collect enough particle mass for chemical analysis. Therefore, it is nearly impossible to obtain real-time or high temporal correlations between chemical species and atmospheric conditions. Furthermore, information on the chemical associations (particle mixing state) cannot be measured with bulk analysis techniques, and one must assume that all particles in the same size range have the same bulk chemical composition [16]. In addition, chemical reactions may occur on or with the filter media during transport and preservation before chemical analysis, thus changing the initially collected aerosol chemical composition [17]. Finally, the gas-particle equilibrium is disturbed by most sampling methods, causing aerosol re-partitioning between different phases; this often causes a bias in the measurement of semivolatile species [18,19]. For example, most filter and impactor techniques operate at pressures below atmospheric pressure. Semivolatile organic compounds particle-to-gas phase transfer may occur under such low pressure conditions.

Real-time single particle mass spectrometry (SPMS) measurements of carbonaceous particles are able to provide unique information on many species by correlating the instantaneous carbonaceous particle composition with rapidly changing atmospheric conditions [20,21]. Many of these techniques are able to obtain both size and chemical composition information on individual particles with high temporal resolution [22–25]. Single particle mass spectral analysis can analyze several particles/second under polluted ambient conditions, allowing for a higher temporal resolution than that which can be achieved using filter-based methods. In addition, the residence time of the single particles in the mass spectrometry instrument is less than 1 ms, minimizing changes in particle morphology and the re-partitioning of chemical species that can occur at reduced pressures. Therefore, SPMS measurements can provide valuable information for studying organic aerosols, as well as semivolatile species. The challenge for SPMS measurements has involved providing quantitative information. One major obstacle is that fluence inhomogeneities in the LDI laser beam utilized by most SPMS measurements result in variations of the ion signal intensities in the mass spectra of identical particles; moreover, instrumental sensitivities to different aerosol components vary with matrix composition [26]. Recently, researchers in multiple labs have begun to explore quantification using SPMS measurements [27–32].

Potassium is a common component of biomass burning particles as observed with filter measurements and electron microscopy with energy-dispersive X-ray spectrometry [33–36]. In recent studies, direct online measurements of biomass aerosols were carried out with other SPMS to investigate the composition and chemical associations of individual biomass particles. Both the particle analysis by laser mass spectrometry (PALMS) and the aerosol time-of-flight mass spectrometry (ATOFMS) measurements observe potassium, organic carbon, and nitrogen-containing species from single particle biomass mass spectra [36,37]. In this work, the time series of biomass burning emission particles and other unique organic particle types in Fresno and Angiola were investigated using an ATOFMS. The unique organic particles, unlike most other particle types detected, display fairly intense peaks between mass-to-charge (m/z) 100 and 200 in the mass spectra and are referred to throughout the paper as high mass organic compounds (HMOC). The possible sources of HMOC particles are described and the temporal variations are presented and discussed. Results from this work will provide useful information on the sources and processes contributing to the organic compounds present in the SJV region as well as other urban areas impacted by high biomass emissions and regional fogs.

2. Experimental

This field campaign was conducted from 30 November 2000 to 4 February 2001 as part of the California Regional Particulate Air Quality Study (CRPAQS). The size and chemical composition of individual particles in the 0.2–3.0 μm size range were measured. The urban Fresno site was located in the center of San Joaquin Valley in a residential neighborhood, and the rural Angiola tower site was located about 80 km southeast of Fresno in the middle of an agricultural area [38]. The results of the measurements taken from 9 January 2001 to 4 February 2001 in Fresno and Angiola are presented in this paper, representing 711,289 particles in Fresno and 614,915 particles in Angiola.

2.1. Data acquisition

The operating principles, design, and performance of the ATOFMS are described in detail elsewhere [39]. Briefly, particles enter the ATOFMS through a converging nozzle and are accelerated to terminal velocities that depend on their aerodynamic diameters, with larger particles traveling slower than smaller particles. Particles then enter a sizing region where they pass through two continuous wave laser beams (diode pumped Nd:YAG at 532 nm) located 6 cm apart. Two scattering signals are collected as each particle passes through the two laser beams. The time difference between the two scattering signals and the distance between the two laser beams are used to calculate the particle velocity, which is converted into particle aerodynamic diameter using a calibration curve determined by polystyrene latex sphere velocities. Particle velocity is also used to calculate the exact time when the particle reaches the source region of the mass spectrometer. A 266 nm Nd:YAG ionization laser is triggered to fire upon particle arrival to produce both positive and negative ions, which are detected by a dual-polarity time-of-flight mass spectrometer. Thus, information on both single particle size and chemical composition can be determined. ATOFMS is particularly efficient at detecting aromatic compounds. Due to the relatively large molar extinction coefficients

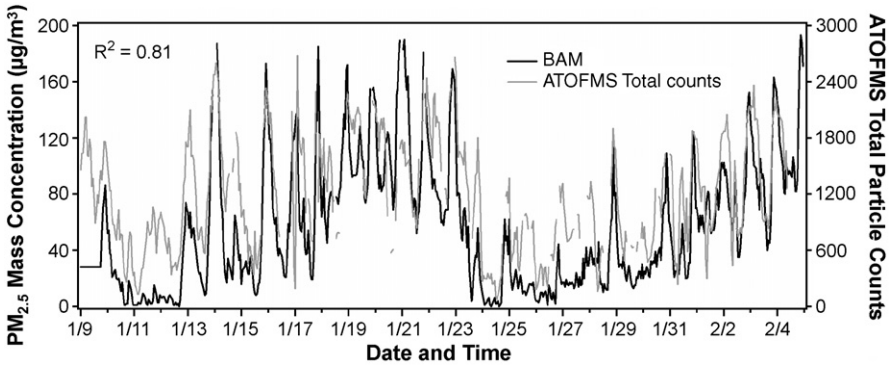

Fig. 1. Time series of ATOFMS total particle counts and $PM_{2.5}$ mass concentration acquired with a beta attenuation monitor (BAM) in Fresno.

at 266 nm ($\varepsilon = 10^3$ to 10^5 L mol^{-1} cm^{-1}) [40,41], mono- and poly-cyclic aromatic hydrocarbons (PAHs) and their derivatives are easily ionized and detected by ATOFMS with high sensitivity. During this study, the ATOFMS ionization laser was operated at reduced power (<1.0 mJ instead of the normal 1.5 mJ) during certain times to study the effect of laser power on ion fragmentation. Due to the fact that particle counts collected within the same amount of time are affected by laser power, reduced power sampling periods are excluded from the discussion and figures.

In this paper, measurements conducted with several other instruments co-located at the Fresno site are also presented for comparison purposes. $PM_{2.5}$ particle mass concentrations were obtained by the Beta Attenuation Monitor (Met One BAM 1020) and total particle-bound PAH concentrations were acquired by photoelectric aerosol sensor (Ecochem Analytics PAS 2000).

2.2. Data analysis

Single particle mass spectra and aerodynamic size information were saved during the field study. A custom software program was used to calibrate the mass spectra and extract a list of ion peaks in the spectra. These peak lists were then imported into YAADA, a single particle mass spectrometry data analysis tool, for further analysis [42].

To obtain a general picture of the aerosol composition over the course of the study, particle information obtained by the ATOFMS is classified using an adaptive resonance theory-based clustering method (ART-2a). ART-2a classifies particles according to the existence and intensity of ion peaks in individual single particle mass spectra and groups particles into the same cluster if they have similar mass spectral fingerprints [43].

3. Results and discussion

3.1. ATOFMS raw counts and mass concentration measurements

The unscaled particle counts obtained directly by the ATOFMS do not represent the ambient particle number concentrations. They can be scaled with other measurements such as a micro-orifice uniform deposit impactor or an aerodynamic particle sizer to obtain quantitative number concentrations [27,30,44,45]. However, for the purposes of this paper, it is important to note that the raw ATOFMS counts show similar variations to those observed with other measurements. Similar agreement between ATOFMS nitrate counts and nitrate mass concentrations from an automated particle nitrate monitor have been shown in previous studies [46]. In this study, hourly temporal variations of ATOFMS total hit particle counts obtained in Fresno and $PM_{2.5}$ mass concentration acquired by the beta attenuation monitor (BAM) are compared in Fig. 1. Data points were excluded if the ATOFMS was offline for more than 30% of a particular hour or low laser power was utilized during that hour. Fig. 1 illustrates the excellent agreement between the time series of the ATOFMS counts and mass concentration measurements: ATOFMS total particle raw counts reach maxima and minima at nearly the same times as the measurements made using the BAM. The fact that ATOFMS raw counts and mass concentrations track one another in this study supports the use of unscaled data to provide an indication of the relative particle concentration changes discussed throughout this paper.

3.2. Mass spectral characteristics of biomass and HMOC in Fresno

After running ART-2a on ATOFMS measurements in Fresno, two unique particle types stood out from all of the other types. The single particle mass spectra of the first type contain a very intense potassium signal (m/z 39) with relatively low intensity positive ion carbonaceous peaks. We refer to the first type as biomass burning particles because non-mineral potassium is a commonly used tracer for wood smoke [47–50]. This biomass particle type accounts for more than 25% of the total analyzed particles, ranging from less than 5% during the day to up to 65% at night. Particles of the second type generally show unique peaks between m/z 100 and 200 in both positive and negative ion spectra in addition to carbonaceous peaks at lower m/z ratios that are similar to biomass type. Specifically, peaks at m/z 115, 128, 139, 153, 165, 178, 189, 202 and peaks at −109, −123, −137, −151, −163, −177, and −191 are the characteristic peaks in these particles. This particle type is referred to as high mass organic carbon (HMOC) particles.

The digital color histograms of the biomass and HMOC particle types are shown in Fig. 2. The y-axis of the digital color histograms represents the fraction of particles for a given parti-

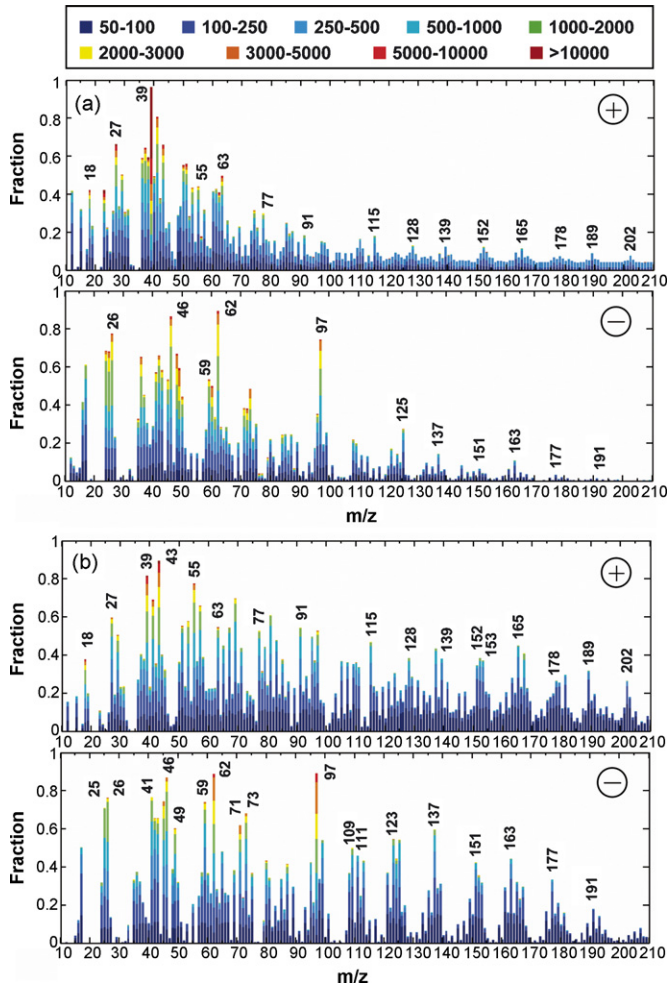

Fig. 2. Digital color stacks of (a) biomass and (b) HMOC particles.

cle type that contain an ion with a peak area within a particular range, as shown in the legend, at each given *m/z* value. Digital color histograms provide valuable information on mass spectral characteristics and the chemical associations for the two particle types. As shown in Fig. 2a, nearly 100% of the biomass particles contain potassium (*m/z* 39) in their positive ion spectra, and 40% of them have extremely intense K^+ signals (area >10,000). A small fraction of the biomass particles (<20%) also contain characteristic HMOC peaks (*m/z* 115, 128, 139, 153, 165, 178, 189, 202, −109, −123, −137, −151, −163, −177, and −191) with very low intensities. The biomass particles show signs of atmospheric aging as indicated by the ammonium marker peak at *m/z* 18 (NH_4^+), nitrate marker ions at −46, −62, and −125 (NO_2^-, NO_3^-, and $HNO_3NO_3^-$), and sulfate ions at −80 and −97 (SO_3^- and HSO_4^-). Some biomass particles (<30%) are associated with mono-aromatic species based on the peaks at *m/z* 77 ($C_6H_5^+$) and *m/z* 91 ($C_7H_7^+$) [51], and polyaromatic compounds indicated by an ion peak at *m/z* 63 [52].

Almost 80% of the HMOC particles also contain a potassium peak as shown in Fig. 2b. The peak at *m/z* 43 is a marker for aged organics and most commonly corresponds to $C_2H_3O^+$ in the ATOFMS; it is the most common peak detected in 90% of the HMOC particles, indicating a higher degree of transformation of the HMOC particles compared to biomass particles. In recent studies in Riverside, the peak at *m/z* 43 is shown to be correlated with highly aged particles and tracks ozone concentrations [53]. There is also the possibility that some fraction of this peak might be due to $C_3H_7^+$ and $C_2H_5N^+$. Additionally, as illustrated in Fig. 2b, approximately 80% of the HMOC particles are associated with levoglucosan, an indicator of biomass burning, which has characteristic peaks at *m/z* −45, −59 and −71 according to the study by Silva et al. [37]. Characteristic HMOC peaks (*m/z* 115, 128, 139, 153, 165, 178, 189, 202, −109, −123, −137, −151, −163, −177, and −191) exist in over 50% of the HMOC particles as shown in Fig. 2b; moreover, the peaks adjacent to the characteristic peaks show high abundances and exist in nearly 40% of the HMOC particles. Interestingly, the peaks appear as a pattern of clusters separated by 12 and 14 *m/z* units (i.e. −109, −123, −137, −151, −165, −179); this type of repetitive pattern is often attributed to oligomers or HULIS species. The HMOC particles are associated with ammonium, nitrate, sulfate, and mono- and poly-cyclic aromatic compounds. A substantial fraction of the HMOC particles (~50%) are also associated with fog processing marker peaks at −81 and −111 (HSO_3^- and $HOCH_2SO_3^-$) [54], suggesting they have undergone some amount of aqueous phase fog processing. A further discussion of this is provided below.

The biomass and HMOC share many common peaks; the major differences are ion peak intensities and the fraction of particles that contain the characteristic markers. As detailed below, the most likely source of the HMOC particles are biomass burning emissions that have partitioned to the particle phase in the cooler evenings and undergone fog processing [55,56].

3.3. Possible assignments of Ion peaks above m/z 100

Definitive assignments for the high *m/z* peaks (*m/z* above 100) are difficult to make a priori since more than one isobar exists for each *m/z* value. In order to make these assignments, information is taken from a combination of previous source characterization studies using filters and ATOFMS, ATOFMS mass spectral fragmentation patterns, ATOFMS lab studies of organic standards, and detailed local emission profiles for the Fresno area. Table 1 lists the most likely assignments. Furthermore, dual ion information and an understanding of the ion peaks produced by a particular organic compound class yields further insight into the peak identification. For example, both protonated and

Table 1
Possible peak assignments for *m/z* above 100

m/z	MW	Most possible assignments
−109	110	Dihydroxybenzene
−123	124	Guaiacol
128	128	Naphthalene
−137, 139	138	Methyl guaiacol
−151, 153	152	Ethy guaiacol/vanillin/acenaphthylene
−163, 165	164	Eugenol
−177, 178, 179	178	Methyl eugenol/phenanthrene/anthracene
202	202	Pyrene/fluoranthene

deprotonated methyl guaiacol peaks are observed by ATOFMS at *m/z* 139 (MH^+) and *m/z* 137 ($M-H^-$) (molecular weight 138). It is possible that instead of being individual compounds, the above peaks are fragment ions of high molecular weight species. In Fresno, more than 50% of the fine organic carbonaceous particles are emitted from residential biomass burning in the winter [6,57]. Schauer and coworkers reported that guaiacols, phenols, and their substituted derivatives accounted for approximately 20% of the total mass of semivolatile gas-phase organic compounds emitted from wood combustion [50]; other studies revealed that biomass burning also emits substantial amounts of methoxyphenols and PAHs [58–62]. It is important to note that the ATOFMS is particularly sensitive to these aromatic compounds due to the use of the 266 nm laser. Thus many of the above peak assignments for peaks above *m/z* 100 are based on the known fragmentation patterns and sensitivity of the ATOFMS technique to specific classes of organic compounds.

3.4. Temporal variations of biomass and HMOC compounds in Fresno

Fig. 3 shows the temporal variations of biomass and HMOC unscaled counts and the percentages of these types measured each hour. Distinct diurnal variations are evident in both biomass and HMOC particles. As shown in Fig. 3a, biomass particle counts/concentrations remain relatively low during the daytime, increase significantly during late afternoon, and reach maxima between 8:00 pm and 3:00 am on most days. The biomass count percentage shows similar diurnal temporal variations. Similar diurnal temporal variations of the HMOC particle counts and count percentages are shown in Fig. 3b. The temporal variations of HMOC and biomass counts track each other very well with a high correlation coefficient of 0.84. The sum of biomass and HMOC particles account for approximately 50% of the total particles detected at night, sometimes even rising above 65%, making them an important fraction of nighttime Fresno aerosol.

3.5. Diurnal trends of biomass particles in Fresno

The distinctive diurnal variations observed for the biomass particles can be explained by a number of factors, including an increase in residential biomass burning activities at night [3,63], accumulation of primary PM emissions, gas/particle phase partitioning of biomass emissions, and a nighttime decrease in the height of the inversion layer. Direct biomass emissions late in the day directly contribute to the observed increase in the ambient biomass aerosols during the evening. Another important factor is gas/particle phase partitioning. Based on partitioning theory, the particle phase concentrations of a particular species will be proportional to its gas phase concentration and the amount of total suspended particulate matter in the atmosphere [64–66]. During the nighttime, both the amount of total suspended particulate matter and biomass emissions increase. Gas phase emissions can partition onto the increased available surface area of the particle phase, increasing the total number of particles that contain biomass emission markers. In addition, lower nighttime temperatures induce semivolatile components to partition to the particle phase. Moreover, other nighttime meteorological conditions further assist in the formation of diurnal variations of biomass particles in Fresno. The nighttime wind speed was low during the study as is typical for winter conditions in the SJV; these stagnant conditions aid in the accumulation of primary emissions. In addition, the lower nighttime inversion layer leads to an increase in the ground level primary particle concentrations. All of these factors contribute to the observed increase in nighttime biomass particle phase concentrations in Fresno, as measured with the ATOFMS.

During the day, direct biomass burning emissions nearly cease. In addition, ambient biomass aerosols and ion markers are transformed and lost during the day through various reactions (i.e. photochemistry) and deposition processes; furthermore, when the inversion layer rises during the day, particles

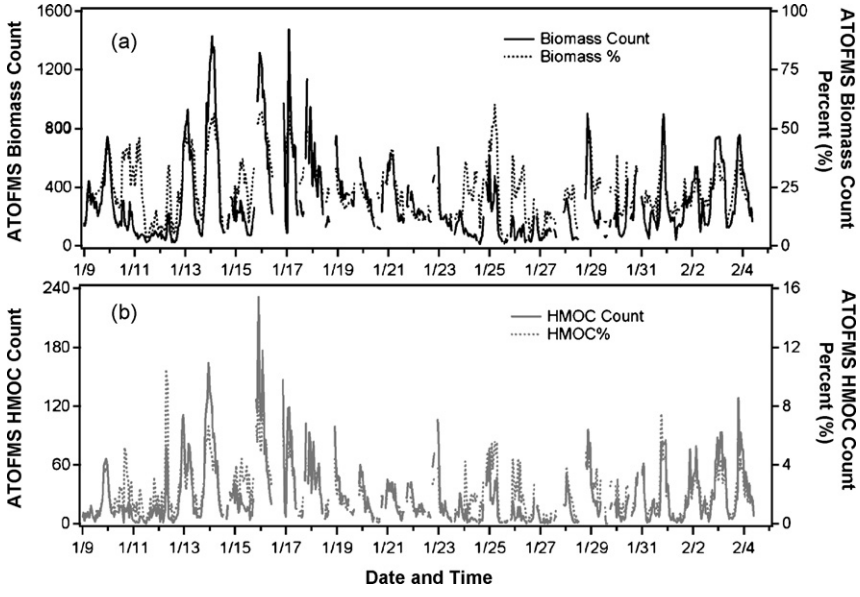

Fig. 3. (a) Time series of ATOFMS biomass particle counts and percentages; (b) time series of ATOFMS HMOC particle counts and percentages.

are released to higher altitudes, causing their concentrations to decrease at ground level. All of these factors contribute to the decrease in biomass particle counts during the daytime.

3.6. Sizes and diurnal variation of HMOC particles in Fresno

The size distributions of the different particle types can provide insight into their sources and formation mechanisms. Hydroxymethanesulfonate ($HOCH_2SO_3^-$, m/z −111) is a known product of fog processing and therefore can be used as an indicator of aqueous phase processing of individual particles [54]. A comparison of the sizes of biomass, HMOC, and fog processed particles (reduced by 3 in order to be shown on the same scale) are presented in Fig. 4. Although biomass and HMOC particle types have very similar temporal variations and many common peaks in their mass spectra, the particle size distributions of these two types differ from one another. The majority of the biomass particles are submicron ($D_a \leq 1.0\,\mu m$) with aerodynamic diameters peaking in the lowest detectable sizes (0.5 μm). Conversely, the HMOC and fog processed particles are primarily supermicron sized particles ($D_a > 1.0\,\mu m$) and have similar size distributions. The respective sizes suggest the biomass particles are directly emitted, whereas the HMOC particles are fog processed and have grown to larger sizes. The similar time series and mass spectra of the HMOC and biomass particles suggest that biomass emissions produce the precursors of the HMOC species that partition to the particles during the night when cooler temperatures and higher RH conditions exist and undergo aqueous phase processing, increasing the size of the processed particles, [67,68].

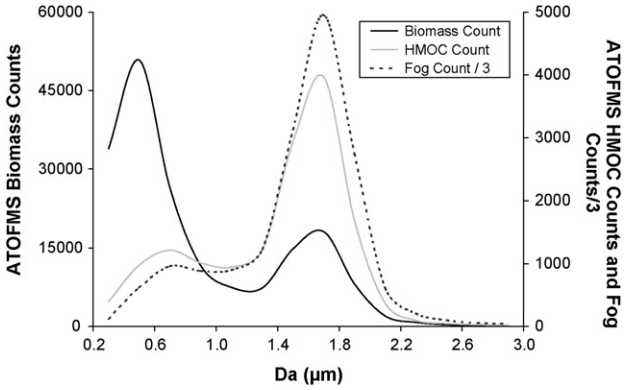

Fig. 4. Size distributions of Fresno biomass, HMOC, and fog processed particles.

Comparing the temporal correlation between HMOC and other species can help identify the sources and factors contributing to their formation. Fig. 5a shows a comparison between the time series of ATOFMS HMOC particle counts and measurements made with a co-located photoelectric aerosol sensor (PAS) at the Fresno site. The signal obtained by the PAS is proportional to the concentration of particle-bound PAHs [69,70], species which are often emitted in biomass emissions [58–60]. ATOFMS HMOC raw particle counts display diurnal variations similar to those observed in PAS measurements. The difference between the two measurements from 19 January to 23 January suggests the presence of other (non-biomass) major PAH

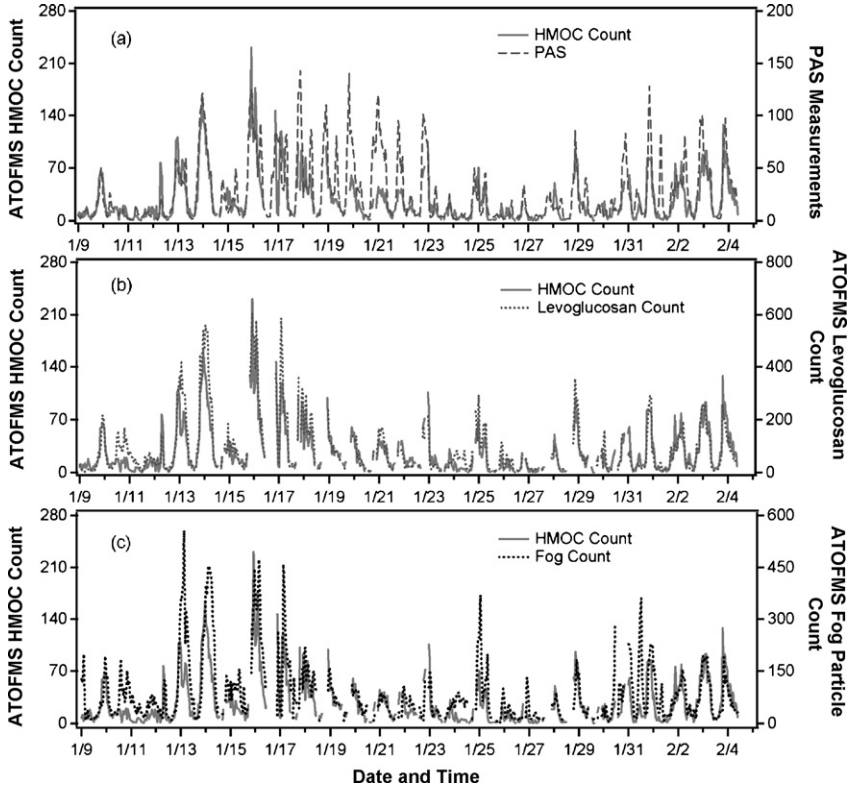

Fig. 5. Time series of (a) HMOC and PAS; (b) HMOC and levoglucosan; (c) HMOC and fog processed particles.

sources. The strong correlations ($R^2 = 0.60$) suggest that HMOC compounds and PAHs are both emitted in biomass emissions. Another useful marker, levoglucosan, has been shown to be a unique marker for wood-smoke aerosols, representing up to 30% of the fine particle organic compound emissions [50,71]. In this analysis, particles containing levoglucosan are selected as those with a relative area of the ion mass signal at each marker peak (m/z −45, −59 and −71) with a relative area of greater than 1%. The temporal variations of HMOC particles and levoglucosan are strongly correlated ($R^2 = 0.84$) as shown in Fig. 5b, this correlation supports the conclusion that the HMOC species in particles in Fresno originate from biomass burning emissions. The correlation between HMOC and fog processed particles are shown in Fig. 5c. The temporal variations of these two particle types reach maxima and minima at about the same time. It is important to note that a substantial fraction of HMOC particles (nearly 50%) contain the fog processing indicator peak at m/z −111, strengthening the conclusion the HMOC species were formed via fog processing. So far the only other ATOFMS field studies where particle types with similar signatures to this HMOC type were observed were two coastal studies where it was hypothesized that these species were formed by aqueous phase processes in cloud droplets during long range transport across the ocean [72]. All the above evidence suggests that the HMOC particles mainly resulted from a combination of biomass emissions, gas/particle partitioning of semivolatile biomass precursors, followed by aqueous phase processing. Previous studies have shown that humic-like substances (HULIS) are generally high mass aromatic compounds with hydroxyl, carboxyl, and carbonyl groups formed in fog/cloud water by oligomerization reactions which were proposed to originate from biomass emissions based on the high concentrations of levoglucosan detected [67,68,73–78]. As described, the HMOC are HULIS most likely formed by aqueous phase reactions from lower molecular weight semivolatile biomass species (for example, methoxyphenols). At this stage, we cannot exclude the possibility that a small fraction of HMOC are HULIS directly emitted from biomass emissions, since HULIS has also been reported to be released from primary biomass emissions [78]. In other studies, ambient photooxidation reactions have also been shown to generate HULIS and oligomeric species, which correlated with O_3 concentration [73,79,80]. In contrast, in the current study, the concentrations of the HMOC particles peaked at night thus indicating that photooxidation was not the dominant formation mechanism.

The diurnal variations of the HMOC particles appear to be most affected by ambient RH and biomass burning emissions in Fresno. During the nighttime, direct biomass emission increases, making more water soluble organic compounds (WSOC) available as the precursor of HULIS [67,74,76]; nighttime low temperature also favors the particle phase partitioning of volatile and semivolatile biomass emissions; high nighttime RH condition (∼90%) substantially increases the liquid water content (LWC) on the particle surface, which can dissolve WSOC and lead to the formation of HULIS through aqueous phase reaction. Thus the diurnal patterns of RH and biomass burning emission lead to a higher HULIS concentration at night, which is observed on ATOFMS as the diurnal temporal variation of HMOC particles. During the daytime, as ambient RH decreases (∼50%), so do biomass burning emissions. Thus much lower HMOC (HULIS) particle counts were detected by the ATOFMS in Fresno during the day.

3.7. Comparison of temporal variations of biomass and HMOC particles in a rural area

It is interesting to compare the single particle results obtained close to the source (Fresno) with those obtained in a distant rural site 80 km away (Angiola). Hourly temporal variations of Angiola biomass particles are presented in Fig. 6. Overall, a much lower average percentage of particles with strong biomass signatures (7%) was measured in Angiola. In general, Angiola biomass particle fractions were below 10% for most of the sampling period but occasionally grew over time to nearly 40%. Fig. 6 illustrates how no obvious diurnal pattern was detected for the Angiola biomass particles. Angiola is located in a remote rural area with very few local emission sources. Thus, the differences in the temporal behavior between Fresno and Angiola are most likely explained by transformations and deposition losses occurring as the biomass particles are transported to Angiola.

It is highly likely that by the time the particles reached Angiola their signatures had evolved to another particle type with a different pattern. This is supported by the observation that rather than having one distinct HMOC type as measured in Fresno, most Angiola particles (>90%) were associated with

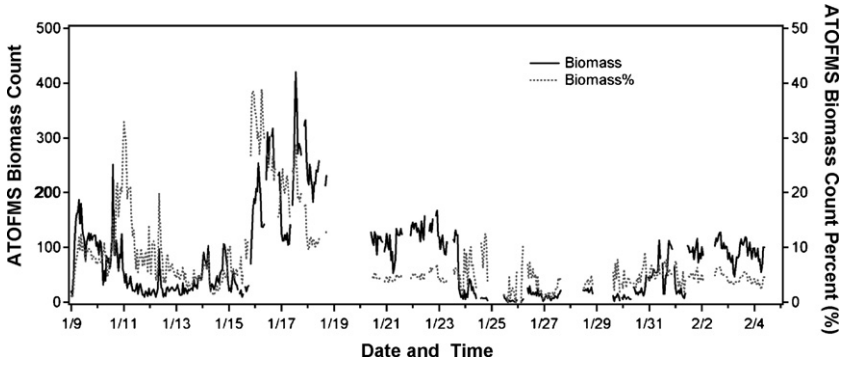

Fig. 6. Time series of biomass particle counts and percentages in Angiola. The particle counts presented here do not include low laser power sampling periods or the periods when the instrument was offline for more than 30% of the hour.

high mass ions, most likely HULIS species, between *m*/*z* 100 and 200 in the positive mass spectra. The presence of these high mass (HULIS) species can be explained by processing occurring during transport. Characteristic high mass ion peaks vary from particle to particle with only a few peaks at the same *m*/*z* as those detected in the Fresno HMOC particle types. Major high mass-to-charge peaks that stand out in the spectra among most Angiola types are *m*/*z* 140, 152, and 160. Negative ion spectra contain a greater amount of nitrate, indicating a higher degree of aging. As particles are transported from different source regions to Angiola, different sources and precursors encountered along the way produce different characteristic high mass peaks.

4. Conclusions

ATOFMS measurements made during the CRPAQS study provide information on particle size, composition, chemical associations, and the temporal variations of biomass burning and HMOC particle types in Fresno and Angiola. Based on a comparison of their size distributions, the larger HMOC particles are most likely HULIS species formed by fog processing. Both time series of the biomass and HMOC particles display a strong diurnal pattern in Fresno, with relatively low daytime particle counts which rapidly increase from late afternoon and peak at night. We hypothesize the diurnal variations are due to an increase in direct biomass emissions followed by gas/particle partitioning of semivolatile species which undergo aqueous phase processing at night. The SJV winter time low inversion layer also contributes to increased levels of these particles at night. In contrast, biomass particles in the rural Angiola area were more heavily transformed, chemically diverse, and show more of a gradual build-up over time. These observations suggest the particle chemistry in Angiola was controlled by long range transport into the area as opposed to by local sources.

The results in this paper demonstrate how single particle measurements can be used to better understand how specific sources and meteorological conditions affect ambient particle mass concentrations. Real-time information on the sizes and temporal variations of biomass and HMOC particles can be used as inputs for models [81] to determine the factors playing the most significant roles in controlling concentrations of organic compounds in the San Joaquin Valley.

Acknowledgements

We thank the California Air Resources Board for financial support (Contract No. 04-336) and the SJV funding agency for supporting CRPAQS.

References

[1] J.R. Whiteaker, D.T. Suess, K.A. Prather, Environ. Sci. Technol. 36 (2002) 2345.
[2] J.G. Watson, J.C. Chow, J. Geophys. Res. Atmos. 107 (2002).
[3] J.G. Watson, J.C. Chow, Atmos. Environ. 36 (2002) 465.
[4] J.S. Lighty, J.M. Veranth, A.F. Sarofim, J. Air Waste Manage. Assoc. 50 (2000) 1565.
[5] J.G. Watson, J.C. Chow, D.H. Lowenthal, L.C. Pritchett, C.A. Frazier, G.R. Neuroth, R. Robbins, Atmos. Environ. 28 (1994) 2493.
[6] J.J. Schauer, G.R. Cass, Environ. Sci. Technol. 34 (2000) 1821.
[7] J.C. Chow, J.G. Watson, D.H. Lowenthal, P.A. Solomon, K.L. Magliano, S.D. Ziman, L.W. Richards, Atmos. Environ. A: Gen. Topics 26 (1992) 3335.
[8] J.D. Blando, B.J. Turpin, Atmos. Environ. 34 (2000) 1623.
[9] K.M. Fahey, S.N. Pandis, J.L. Collett, P. Herckes, Atmos. Environ. 39 (2005) 4561.
[10] J.C. Chow, J.G. Watson, D.H. Lowenthal, P.A. Solomon, K.L. Magliano, S.D. Ziman, L.W. Richards, Aerosol Sci. Technol. 18 (1993) 105.
[11] J.C. Chow, J.G. Watson, E.M. Fujita, Z.Q. Lu, D.R. Lawson, L.L. Ashbaugh, Atmos. Environ. 28 (1994) 2061.
[12] L.W. Richards, S.H. Alcorn, C. McDade, T. Couture, D. Lowenthal, J.C. Chow, J.G. Watson, Atmos. Environ. 33 (1999) 4787.
[13] C.L. Blanchard, P.M. Roth, S.J. Tanenbaum, S.D. Ziman, J.H. Seinfeld, J. Air Waste Manage. Assoc. 50 (2000) 2073.
[14] B.J. Turpin, P. Saxena, E. Andrew, Atmos. Environ. 34 (2000) 2983.
[15] S.N. Pandis, A.S. Wexler, J.H. Seinfeld, J. Phys. Chem. 99 (1995) 9646.
[16] T.A. Cahill, P. Wakabayashi, Adv. Chem. Ser. (1993) 211.
[17] X.Q. Zhang, P.H. McMurry, Atmos. Environ. 21 (1987) 1779.
[18] J. Volckens, D. Leith, Environ. Sci. Technol. 36 (2002) 4613.
[19] J. Volckens, D. Leith, Atmos. Environ. 37 (2003) 3177.
[20] C.A. Noble, K.A. Prather, Geophys. Res. Lett. 24 (1997) 2753.
[21] S.A. Guazzotti, J.R. Whiteaker, D. Suess, K.R. Coffee, K.A. Prather, Atmos. Environ. 35 (2001) 3229.
[22] K.P. Hinz, R. Kaufmann, B. Spengler, Anal. Chem. 66 (1994) 2071.
[23] K.A. Prather, T. Nordmeyer, K. Salt, Anal. Chem. 66 (1994) 1403.
[24] P.J. McKeown, M.V. Johnston, D.M. Murphy, Anal. Chem. 63 (1991) 2069.
[25] D.M. Murphy, D.S. Thomson, Aerosol Sci. Technol. 22 (1995) 237.
[26] B.A. Mansoori, M.V. Johnston, A.S. Wexler, Anal. Chem. 66 (1994) 3681.
[27] X. Qin, P.V. Bhave, K.A. Prather, Anal. Chem. 78 (2006) 6169.
[28] J.O. Allen, P.V. Bhave, J.R. Whiteaker, K.A. Prather, Aerosol Sci. Technol. 40 (2006) 615.
[29] D.A. Lake, M.P. Tolocka, M.V. Johnston, A.S. Wexler, Environ. Sci. Technol. 37 (2003) 3268.
[30] P.V. Bhave, J.O. Allen, B.D. Morrical, D.P. Fergenson, G.R. Cass, K.A. Prather, Environ. Sci. Technol. 36 (2002) 4868.
[31] D.A. Sodeman, S.M. Toner, K.A. Prather, Environ. Sci. Technol. 39 (2005) 4569.
[32] R.C. Moffet, L.G. Shields, J. Bernstsen, R.B. Devlin, K.A. Prather, Aerosol Sci. Technol. 38 (2004) 1123.
[33] J. Li, M. Posfai, P.V. Hobbs, P.R. Buseck, J. Geophys. Res. Atmos. 108 (2003).
[34] M. Posfai, R. Simonics, J. Li, P.V. Hobbs, P.R. Buseck, J. Geophys. Res. Atmos. 108 (2003).
[35] X.D. Liu, P. Van Espen, F. Adams, J. Cafmeyer, W. Maenhaut, J. Atmos. Chem. 36 (2000) 135.
[36] P.K. Hudson, D.M. Murphy, D.J. Cziczo, D.S. Thomson, J.A. de Gouw, C. Warneke, J. Holloway, J.R. Jost, G. Hubler, J. Geophys. Res. Atmos. 109 (2004).
[37] P.J. Silva, D.Y. Liu, C.A. Noble, K.A. Prather, Environ. Sci. Technol. 33 (1999) 3068.
[38] J.G. Watson, J.C. Chow, J.L. Bowen, D.H. Lowenthal, S. Hering, P. Ouchida, W. Oslund, J. Air Waste Manage. Assoc. 50 (2000) 1321.
[39] E. Gard, J.E. Mayer, B.D. Morrical, T. Dienes, D.P. Fergenson, K.A. Prather, Anal. Chem. 69 (1997) 4083.
[40] I.B. Berlman, Handbook of Fluorescence Spectra of Aromatic Molecules, 2nd ed., Academic Press, New York, 1971.
[41] B.J. Finlayson-Pitts, J.N. Pitts Jr., Chemistry of the Upper and Lower Atmosphere: Theory, Experiments, and Applications, Academic Press, San Diego, CA, 2000.
[42] J.O. Allen, Arizona State University, 2002, http://www.yaada.org.
[43] X.H. Song, P.K. Hopke, D.P. Fergenson, K.A. Prather, Anal. Chem. 71 (1999) 860.

[44] J.O. Allen, D.P. Fergenson, E.E. Gard, L.S. Hughes, B.D. Morrical, M.J. Kleeman, D.S. Gross, M.E. Galli, K.A. Prather, G.R. Cass, Environ. Sci. Technol. 34 (2000) 211.
[45] D.T. Suess, K.A. Prather, Chem. Rev. 99 (1999) 3007.
[46] D.Y. Liu, K.A. Prather, S.V. Hering, Aerosol Sci. Technol. 33 (2000) 71.
[47] K. Sexton, K.S. Liu, S.B. Hayward, J.D. Spengler, Atmos. Environ. 19 (1985) 1225.
[48] A.E. Sheffield, G.E. Gordon, L.A. Currie, G.E. Riederer, Atmos. Environ. 28 (1994) 1371.
[49] W.C. Malm, K.A. Gebhart, J. Air Waste Manage. Assoc. 47 (1997) 250.
[50] J.J. Schauer, M.J. Kleeman, G.R. Cass, B.R.T. Simoneit, Environ. Sci. Technol. 35 (2001) 1716.
[51] P.J. Silva, K.A. Prather, Anal. Chem. 72 (2000) 3553.
[52] F. McLafferty, M. Turecek, F. Turecek, Interpretation of Mass Spectra, 4th ed., University Science Books, 1993.
[53] X. Qin, L.G. Shields, S.M. Toner, K.A. Prather, in preparation.
[54] J.R. Whiteaker, K.A. Prather, Atmos. Environ. 37 (2003) 1033.
[55] O.L. Mayol-Bracero, P. Guyon, B. Graham, G. Roberts, M.O. Andreae, S. Decesari, M.C. Facchini, S. Fuzzi, P. Artaxo, J. Geophys. Res. Atmos. 107 (2002).
[56] B. Graham, O.L. Mayol-Bracero, P. Guyon, G.C. Roberts, S. Decesari, M.C. Facchini, P. Artaxo, W. Maenhaut, P. Koll, M.O. Andreae, J. Geophys. Res. Atmos. 107 (2002).
[57] M.W. Poore, J. Air Waste Manage. Assoc. 52 (2002) 3.
[58] H.H. Yang, C.H. Tsai, M.R. Chao, Y.L. Su, S.M. Chien, Atmos. Environ. 40 (2006) 1266.
[59] S.S. Xu, W.X. Liu, S. Tao, Environ. Sci. Technol. 40 (2006) 702.
[60] M. Mandalakis, O. Gustafsson, T. Alsberg, A.L. Egeback, C.M. Reddy, L. Xu, J. Klanova, I. Holoubek, E.G. Stephanou, Environ. Sci. Technol. 39 (2005) 2976.
[61] P.M. Lemieux, C.C. Lutes, D.A. Santoianni, Prog. Energy Combust. Sci. 30 (2004) 1.
[62] J. Kjallstrand, O. Ramnas, G. Petersson, Chemosphere 41 (2000) 735.
[63] J.C. Chow, J.G. Watson, D.H. Lowenthal, R. Hackney, K. Magliano, D. Lehrman, T. Smith, J. Air Waste Manage. Assoc. 49 (1999) 16.
[64] J.F. Pankow, L.M. Isabelle, D.A. Buchholz, W.T. Luo, B.D. Reeves, Environ. Sci. Technol. 28 (1994) 363.
[65] M. Jang, R.M. Kamens, K.B. Leach, M.R. Strommen, Environ. Sci. Technol. 31 (1997) 2805.
[66] B.T. Mader, J.F. Pankow, Environ. Sci. Technol. 36 (2002) 5218.
[67] A. Hoffer, G. Kiss, M. Blazso, A. Gelencser, Geophys. Res. Lett. 31 (2004).
[68] J.S. Feng, D. Moller, J. Atmos. Chem. 48 (2004) 217.
[69] H. Burtscher, J. Aerosol. Sci. 23 (1992) 549.
[70] J.C. Dunbar, C.I. Lin, I. Vergucht, J. Wong, J.L. Durant, Sci. Total Environ. 279 (2001) 1.
[71] B.R.T. Simoneit, J.J. Schauer, C.G. Nolte, D.R. Oros, V.O. Elias, M.P. Fraser, W.F. Rogge, G.R. Cass, Atmos. Environ. 33 (1999) 173.
[72] J.C. Holecek, S.M. Toner, K.A. Prather, in preparation.
[73] V. Samburova, S. Szidat, C. Hueglin, R. Fisseha, U. Baltensperger, R. Zenobi, M. Kalberer, J. Geophys. Res. Atmos. 110 (2005).
[74] M.C. Facchini, S. Fuzzi, S. Zappoli, A. Andracchio, A. Gelencser, G. Kiss, Z. Krivacsy, E. Meszaros, H.C. Hansson, T. Alsberg, Y. Zebuhr, J. Geophys. Res. Atmos. 104 (1999) 26821.
[75] Z. Krivacsy, G. Kiss, B. Varga, I. Galambos, Z. Sarvari, A. Gelencser, A. Molnar, S. Fuzzi, M.C. Facchini, S. Zappoli, A. Andracchio, T. Alsberg, H.C. Hansson, L. Persson, Atmos. Environ. 34 (2000) 4273.
[76] Z. Krivacsy, A. Gelencser, G. Kiss, E. Meszaros, A. Molnar, A. Hoffer, T. Meszaros, Z. Sarvari, D. Temesi, B. Varga, U. Baltensperger, S. Nyeki, E. Weingartner, J. Atmos. Chem. 39 (2001) 235.
[77] A. Gelencser, A. Hoffer, G. Kiss, E. Tombacz, R. Kurdi, L. Bencze, J. Atmos. Chem. 45 (2003) 25.
[78] E.R. Graber, Y. Rudich, Atmos. Chem. Phys. 6 (2006) 729.
[79] D.S. Gross, M.E. Galli, M. Kalberer, A.S.H. Prevot, J. Dommen, M.R. Alfarra, J. Duplissy, K. Gaeggeler, A. Gascho, A. Metzger, U. Baltensperger, Anal. Chem. 78 (2006) 2130.
[80] M. Kalberer, D. Paulsen, M. Sax, M. Steinbacher, J. Dommen, A.S.H. Prevot, R. Fisseha, E. Weingartner, V. Frankevich, R. Zenobi, U. Baltensperger, Science 303 (2004) 1659.
[81] T. Held, Q. Ying, A. Kaduwela, M. Kleeman, Atmos. Environ. 38 (2004) 3689.